Analysing the Impact of Process Dependent Thermal Loads on the Prediction Accuracy of Thermal Effects in Machine Tool Components

Eric Wenkler[1,2(✉)], Christoph Steiert[1], Eugen Boos[1], and Steffen Ihlenfeldt[1,2]

[1] TU Dresden, Institute of Mechatronic Engineering, 01062 Dresden, Germany
eric.wenkler@tu-dresden.de

[2] Fraunhofer Institute for Machine Tools and Forming Technology IWU, 01069 Dresden, Germany

Abstract. Thermal changes are one major reason for machining errors. The simulation of thermal compensation processes is therefore of extraordinary importance for the correction and compensation of thermal errors. Most models assume static power losses in machine components and neglect the influence of the machining task on the resulting power losses. Previews research showed that the machine tool activity has a significant effect on occurring power losses. Coupled to a FE model, thermal errors can be predicted more accurately. To investigate the advantages and disadvantages of this approach, the procedure was applied and examined on a machine basis, which is one of the most complex components of a machine tool from a thermal point of view. Therefore, this work describes the concept, application and evaluation of the task-specific thermal prediction. The paper showed that this strategy allows the extrapolation to an unknown and complex load scenario with only 30% prediction error.

Keywords: Machine Tool · Temperature · FEM · Automation

1 Introduction

Machine tools are the core manufacturing system for an efficient machining of high-quality parts. Their accuracy and performance drastically increased within the last decades, and with that the major problem domain shifted from limited positioning accuracy and stiffness to thermally caused positioning errors. It is assumed that more than half of all machining errors is caused by thermal effects [1]. Because of this reason, high effort is put on the compensation and correction of thermal errors. Compensational approaches try to minimize the thermal sensitivity of the machine tool by integrating passive or active elements, while correctional approaches attempt to estimate thermal errors and minimize them by considering the thermal error within the machine tool control as dynamic position offset. First, compensational approaches are discussed, which can further be divided in passive and active.

S. Ihlenfeldt (Ed.): ICTIMT 2023, LNPE, pp. 99–115, 2023.
https://doi.org/10.1007/978-3-031-34486-2_8

Passive compensational approaches are mainly achieved by the integration of thermally resistant materials, which are chosen for example by their conductivity, heat capacity or expansion coefficient. Möhring et al. gave a broad overview of developments in machine tool relevant materials [2]. A typical example is the use of stone and ceramic composites for machine bases. Such thermally and mechanically resistant materials are mainly used as carrier material for unmoved parts in the machine tool. Another recent example for a passive compensation approach is examined by Voigt et al., who attached phase changing materials to the nut of a ball screw drive [3]. If the phase change temperature is reached, the material changes its structure and with that increases its heat capacity significantly. This raises the heat capacity of the whole assembly and reduces further thermal changes.

On the other side are active compensational approaches, which characterize by a requirement for additional energy. Typical solutions for this group are fluid based cooling systems, which are state of the art for modern machine tools. Basic fluid cooling systems start with the machine tool and continuously pump fluid through lossy assemblies to remove the heat and prevent the assembly from excessive heating. Since the convective heat transfer raises in efficiency with increasing temperature difference, most cooling systems are fully active or 2-point controlled, which means that they start when a predefined temperature is reached in the assembly. This prevents the cooling system of consuming energy in case of minor temperature differences, where no significant heat removal can be achieved. Mori et al. applied this approach to a spindle cooling system and showed that energy savings from 15% to 75% can be achieved, depending on the operational state of the spindle [4]. Recent research shows a great potential in volume flow controlled cooling systems [5, 6]. If a thermal difference between assembly and coolant tank is given, the volume flow of the cooling system can be changed to maintain the machine tool temperature at a specified value. Such a thermal difference can be achieved by using a compressor or allowing higher temperatures in the machine tool.

The second major group are correctional approaches, which characterize by accepting the thermo-elastic error and correct it together with the machine tool control. Therefore, the precise measurement or prediction of thermo-elastic displacements is of high priority. Finite element (FE) based simulations are most common in this field, since they are able to consider nearly all physical effects, relevant for thermal changes. The greatest disadvantage in FE based simulations is the high effort, required to obtain an accurate simulation [7]. Especially for machine tools, such simulations require major effort, since a machine tool includes multiple assemblies, which additional may have losses and change their position with time (e.g. X-Axis position). This requires a dynamically connected model to consider positional changes and additional a great experimental effort to determine losses, which may also change depending on the assembly's operational state. Further heat transfer properties at the joints between assemblies must be determined, which is practically only possible by disassembling the whole machine tool with major experimental setups.

Because of the great effort required for a machine tool FE model, alternative approaches are researched, to predict thermo-elastic effects. A typical alternative is the determination of characteristic maps and their use for thermal predictions [8]. Such

approaches are mostly data driven and do not consider physical mechanisms of heat transfer. Therefore, their ability for inter- and extrapolation is strongly limited.

In nearly all forecast strategies, the task caused change in power loss of lossy machine tool assemblies is not considered. Instead, average losses are measured and used. Previous research showed that the manufacturing task (G-code) greatly effects losses and with that the resulting temperature [9, 10]. According to this finding, this paper describes the creation of a FE model, capable to consider the varying and task specific heat introduction.

2 Research Overview

The focus of this research is the consideration of task dependent losses in machine tools to increase the accuracy of FE predictions. Since complete machine tool models require great effort in finite element model (FEM) creation and adjustment of model parameters, a machine basis was used as research object. This reduces the effort for the FEM creation, which is not in focus of this paper. The chosen machine basis is a unique basis build for research of tempering strategies and does not belong to a real machine tool. Since no lossy assemblies are mounted, heating pads were attached, to simulate such lossy assemblies. Figure 1 shows a picture of the machine basis, that is equipped with 20 heating pads, 7 cooling circuits and 30 temperature sensors. Its core material is made up of Hydropol [11], with steel casing and reinforcement. It has a width of 1.4 m, a depth of 2 m and a height of 1.6 m.

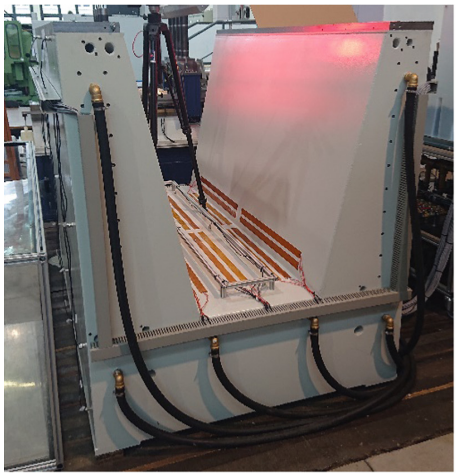

a) Photo of the machine basis

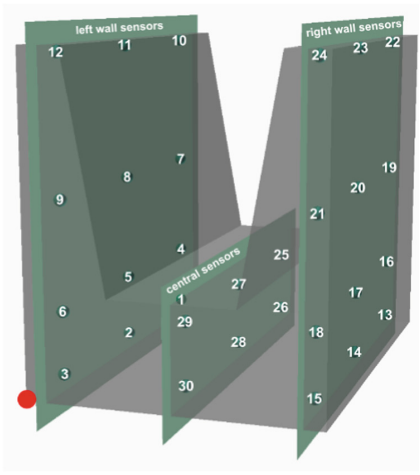

b) Integrated sensor locations

Fig. 1. Research object: machine basis

The abstract procedure for creating a FE Simulation, that considers task specific varying thermal loads is illustrated in Fig. 2. It implies the creation of a model, the optimization of parameters to improve model accuracy and the accurate prediction of thermal

loads, used as bounding conditions for the FEM. The paper describes the application and analysis of this approach for the machine basis as demonstrator.

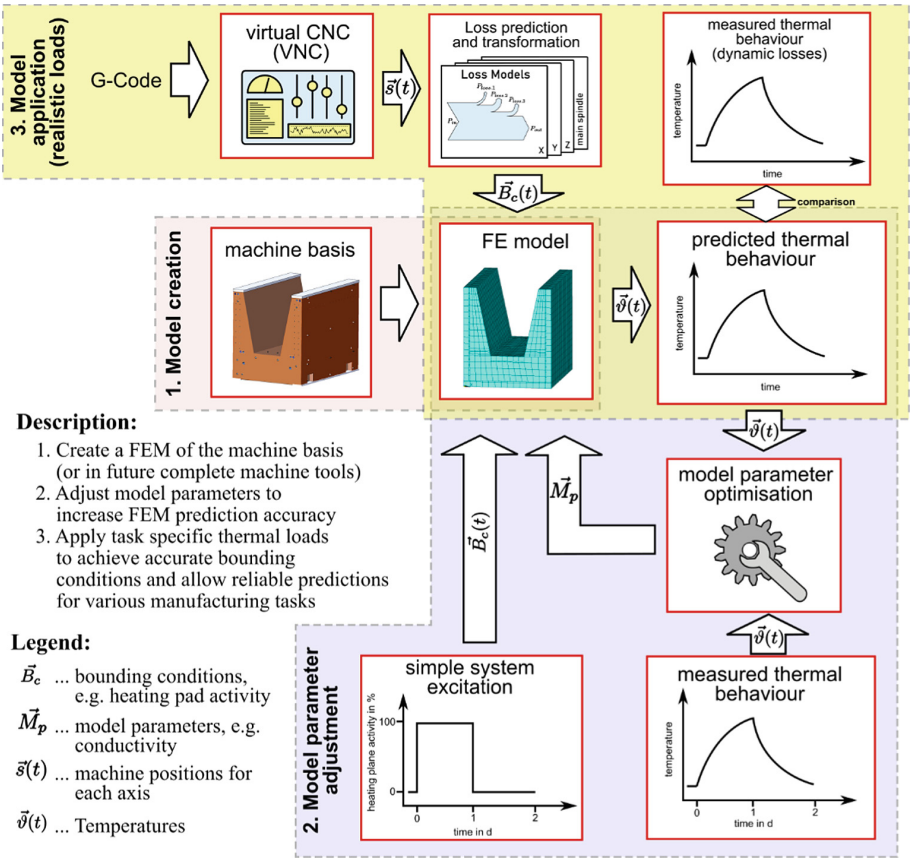

Fig. 2. Abstract overview to the application of task dependent loads in FEM

3 Finite Element Model

3.1 General Procedure of Thermal Error Estimation

Accurate thermal and thermo-elastic predictions are of major importance in the field of machine tools. Deviations between expected and real temperatures lead to positional deviations and therefore directly affect the manufacturing quality. Common approaches for thermal predictions focus on the physical simulation of heat transfer processes, which is mostly achieved with the use of finite element models (FEM) or finite difference models (FDM). These models discretize the body of the simulation object and calculate the heat transfer mechanisms for small and easy shaped elements with the use of basic heat transfer equations.

The accuracy of such approaches depend on two major points:

- **Model quality:** The simulation is always abstracted and cannot be as accurate as the real object. For example, the model discretization strongly effects the simulation accuracy and the computing effort, which is why a trade-off between simulation speed and accuracy is necessary. Further it is common to ignore small geometrical features, that are assumed to have no impact, but consequently they lead to slight deviations and the sum of such simplifications can lead to major deviations. Therefore, the simulation model contains a base error that cannot be overcome.
- **Boundary condition quality:** The boundary conditions define the excitation of the system. The simulation model takes them and computes heat transfer processes. Incomplete or inaccurate boundary conditions lead to wrong excitations of the system and therefore to wrong simulation results. According to this, it is from major importance to achieve as realistic boundary conditions as possible.

Especially boundary conditions for internal heat sources are often abstracted in thermal simulations of machine tools and their correlation to the machining task is not considered. It is a common procedure to create a thermal simulation, define boundary conditions at areas where heat is expected, like motors or bearings, and perform measures to calibrate the power loss for the specific boundary condition. Such tests are mostly done by performing trivial machine movements, like repetitive linear movements of the machine axes, as done in thermal stability measures normed in ISO 230-3. This strongly deviates from the machine movement under production conditions, which is very task dependent. Since the emitted power losses in active machine assemblies strongly depend on their operational state (e.g., the rotational speed of a feed axis bearing), a static power loss, as assumed in most models, leads to major simulation deviations. This reasons the following investigation on the consideration of task dependent loads within FEM.

The following sections describe the creation (Sect. 3.2) and optimization (Sect. 3.3) of the FEM, for a later application of task dependent loads.

3.2 FE Model Creation

The model for the machine basis was created with Ansys APDL (**A**nsys **P**arametric **D**esign **L**anguage), which is the original Ansys application. The script support allows a graphicly guided development and debug of the model, but also the automated execution in background. The capability for automated execution will be used for an optimization of model parameters within the next Sect. 3.3. Figure 3 gives a general introduction to the created model. The major geometrical features of the machine basis were considered during the recreation within Ansys. To force the creation of Nodes at positions with bounding conditions, the initial body was cut multiple times (see Fig. 3a). The resulting volumes were roughly meshed with an edge size of 100 mm. This in fact leads to a rough model with limited accuracy, but significantly decreases the computation time, which will already be big according to the transient simulation.

The model considers three bounding conditions, which are:

1. **Fluid circuits:** The machine basis has 7 separate cooling circuits, which are individually controlled. These circuits were modelled with 1D-Fluid-Elements as illustrated

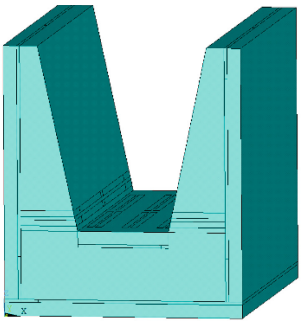

a) Geometry of the machine basis

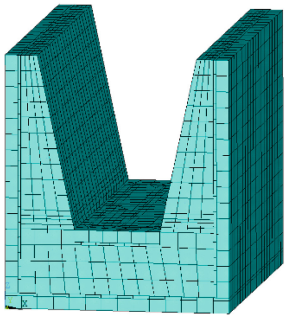

b) Generated mesh for the FEM

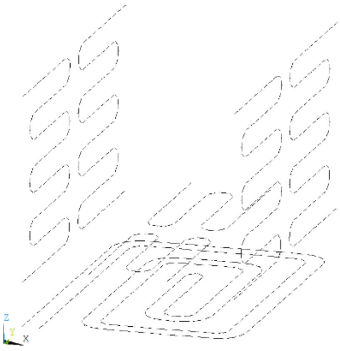

c) Fluid circuit (1D-Elements)

d) Heating pads for heat introduction

Fig. 3. Created FE-Model

in Fig. 3c. The elements can be controlled by defining volume flow and fluid inlet temperature.

2. **Heating pads:** In the central area of the machine basis are 20 heating pads mounted. Each wall is attached with 4 pads, while 12 pads are mounted in the central (horizontally oriented) surface (see Fig. 1 or 13). Therefore 20 bounding conditions were added to the model, with a controllable heat flow through each of the 20 surfaces.
3. **Convection:** Since the heat exchange to the environment is an important heat sink for the model, convection was defined at all outer surfaces of the model. For simplification the heat transfer coefficient α was assumed to be equal at each surface.

The activity of a bounding condition can be set from outside over an CSV file, which is passed to the model and read during simulation start. With this setup, the model can efficiently be applied to various load scenarios, which is important for further practical applications.

It is to mention that the presented model is a rough model, only considering major thermal impacts. The geometry is simplified and inner steal inlets for reinforcement are not modelled. Effects like the varying heat transfer coefficient over the surface, or the radiation with the environment could have increased the model accuracy, but also

require a huge experimental effort. Since the goal is to generally show the possibility for predicting the thermal behaviour in machine components, with consideration of the task, such high-effort-low-gain effects were neglected.

3.3 Automated Optimization of FEM Parameters

The created model was initialized with default material properties obtained from common material tables. Together with the geometrical simplification of the model, simulation errors are unavoidable. Since all models are a simplification of the real object, it is a common approach to adjust model parameters to increase the model accuracy [7]. Therefore, simple load cases were prepared and applied to the machine basis, to measure the real thermal behaviour and use it for a model parameter optimization, as illustrated in Fig. 2. One reference measure was taken for the heating with heating pads and one for the cooling with the cooling system. Within these test cases, all heating pads/cooling-circuits were fully active for one day, and then turned off to measure the harmonization behaviour for one additional day. For simplification, the focus is put on the heating pads while the cooling system is not considered. For consistency it is to mention, that the following parameter adjustment procedure is identical for heating pads and cooling circuits.

The adjustment of model parameters based on thermal measures is an iterative task since discrete models as FEM do not allow a direct quantification of the thermal impact of a specific parameter. In fact, if a parameter is changed, the whole simulation must be repeated, to compare results and quantify the impact of the model parameter and decide how to adjust a parameter. Since this is the core intention of mathematical optimization approaches, an optimizer was implemented for the model parameter adjustment.

The optimizer takes a set of parameters with bindings, that he is allowed to adjust, and repetitively executes the FE model with different parameters, to quantify the impact on the model and decide how to adjust parameters to minimize the model error. Since optimizers try to minimize a scalar error value, the computation of an error value was required, that represents the error between the measured and simulated temperature curves over each 30 sensors. Therefore, Eq. 1 was used as cost function, which represents the mean square error (MSE). Parameters are: number of sensors s, number of simulated/measured time steps l (must be equal), simulated temperatures S and measured temperatures M.

$$E = \frac{\sum_{n=1}^{s} \sum_{m=1}^{l} (S_{m.n} - M_{m.n})^2}{s \cdot l} \tag{1}$$

MSE is a common cost function that aims to globally fit the curves. According to the square of the difference, great differences have a huge impact on the overall error, while minor differences have a small one. Therefore, MSE will always lead to slight deviations since local error maxima have the main influence on the total error, that are reduced on cost of places with small errors.

The used optimizer was COBYLA (**C**onstrained **O**ptimization **B**y **L**inear **A**pproximation), which showed the best performance and a fast convergence under 10 tested gradient free optimizers. The test was performed by comparing the simulation

time and final MSE, achieved after 50 optimization steps by providing the simple system excitation together with the measured behaviour (see Fig. 4 block 1). Figure 4 shows a more detailed overview of the implemented optimization procedure.

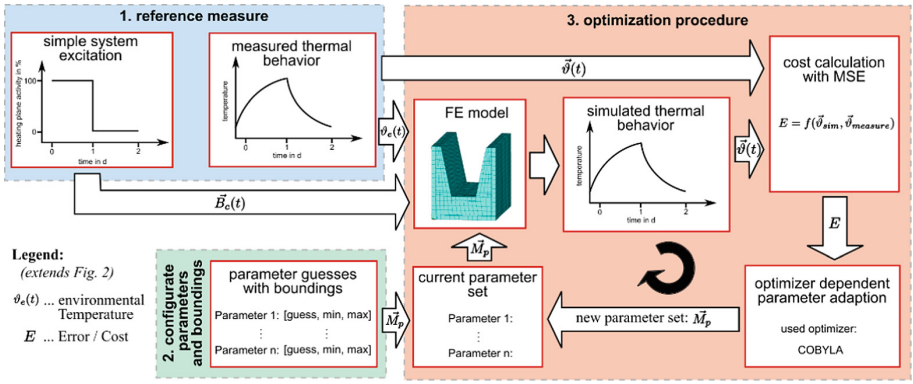

Fig. 4. Block diagram showing the procedure for parameter optimization

Table 1. Optimization configuration and result

Parameter	Unit	Start value	Minimum	Maximum	Optimum
Power of heating pad	W	45	0	50	49.3
Air conv. Coefficient	$W\ m^{-2}\ K^{-1}$	10	8	100	12.1
Hydropol conductivity	$W\ m^{-1}\ K^{-1}$	6.2	6.2	50	6.2
Hydropol density	$kg\ m^{-3}$	2450	2450	7850	4588.4
Hydropol heat capacity	$J\ kg^{-1}\ K^{-1}$	980	470	980	979.2

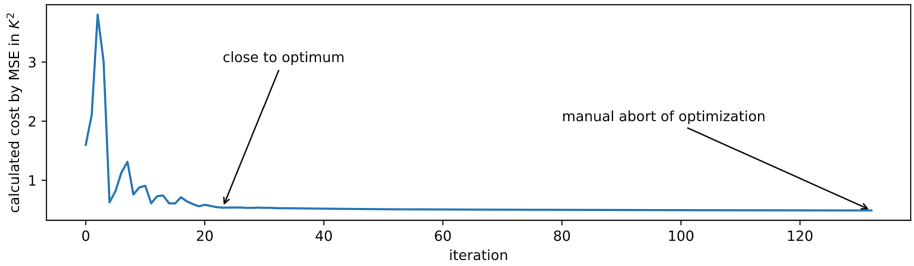

Fig. 5. Cost (MSE) development during optimization procedure

The optimization was started with default parameters (see Table 1). The bindings were set, so that the parameters remain within the range between Hydropol and steal, since the steel inlets were not modelled, and optimal parameters may move in between. According to Fig. 5, the MSE dropped from 1.60 K^2 to 0.53 K^2 after already 20 iterations.

The optimization was manually aborted with a final MSE of 0.48 K^2, which describes an average prediction error reduction from 1.26 K to 0.69 K. Even if this reduced the range of absolute errors from [−1.54 K, 3.2 K] to [−1.5 K, 2 K], some local errors increased (compare Fig. 6 and 7). This normally occurs when the model capacity is reached, forcing the optimizer to start with the error distribution, to minimize the cost criteria. Therefore, a further error reduction could be achieved with a more detailed model.

At this point the model is created and parameters are improved to achieve maximum correlation between reality and simulation, allowing the application of process dependent loads.

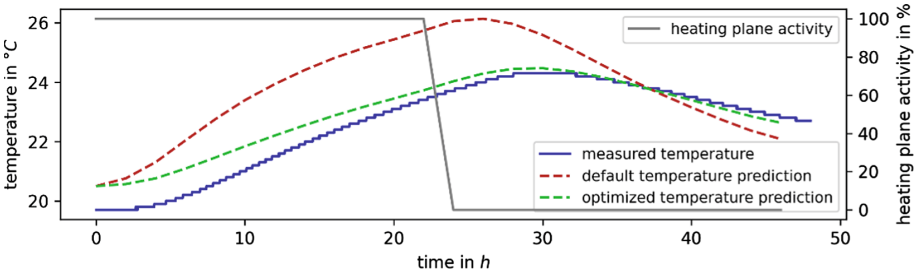

Fig. 6. Exemplary local accuracy increase by global parameter adjustment (Sensor 26)

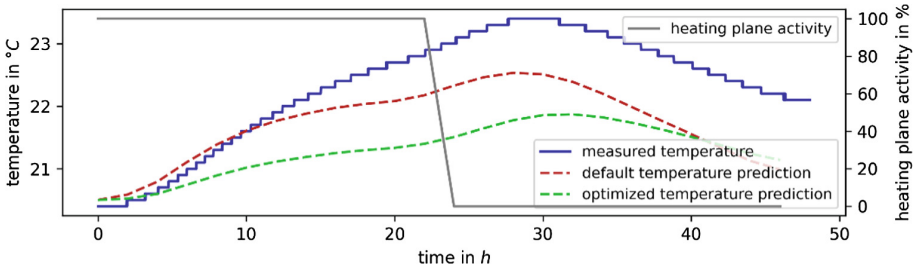

Fig. 7. Exemplary local accuracy decrease by global parameter adjustment (Sensor 19)

4 Obtain Manufacturing Task Characteristic Thermal Loads

The determination of thermal loads that come with a manufacturing task (G-code) requires the interpretation of the G-code, to determine resulting movements and apply axis specific loss models. This procedure was analysed in [9, 10] and its application, to estimate realistic thermal loads for the FEM, is described in this section.

4.1 Reference Task for Realistic Load Scenario

Realistic thermal loads can be achieved by the usage of a typical industrial manufacturing task. Therefore, a part was constructed that is characteristic for the field of aerospace,

which mainly requires the parts to be light and stable. Since sheet metal constructions do not achieve the required stability, the parts are mostly manufactured from the solid and have great volume reduction rates above 80%.

Figure 8 shows the constructed part that is typical for support structures as used in pads, rockets or satellites. Its main dimensions are 504 × 291 × 140 mm and the corresponding raw part dimensions are 514 × 310 × 150 mm. Only 6% of the initial material remain in the final part. The planned technology includes only the first clamping, which is for the upper half of the part and contains a roughing and two finishing operations. A third and final finishing operation is assumed to be performed at the end of the second clamping, which is therefore not considered here. The many finishing operations are essential, since residual stress is released during the material removal, leading to a part deformation, and therefore requiring a slow iteration down to the final part geometry. Figure 8 summarizes the technological steps used for the considered first clamping process.

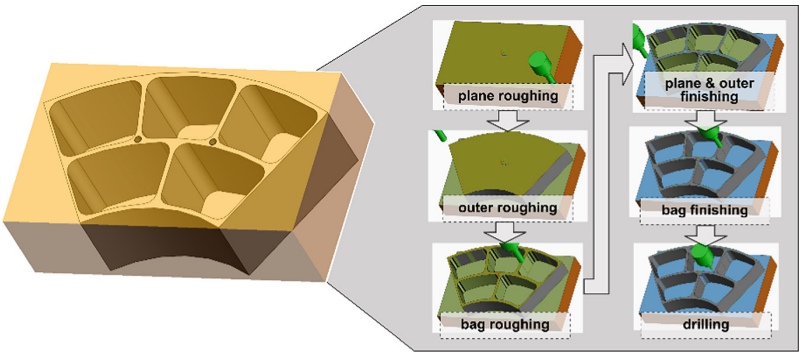

Fig. 8. Reference task and prepared technology (process steps)

4.2 Task Characteristic Power Loss Estimation

The estimation of task characteristic power losses was already developed for a hexapod in previous research [9, 10], which will be reused for this approach. The solution interprets the G-Code with the use of a virtual numerical control (VNC) that mimics the real control of the machine tool. Consequently, the machine movement can be predicted, which further allows the application of power loss models to estimate power losses within the machine tools lossy assemblies (see Fig. 9).

Most machine tools have a serial kinematic, since the general accuracy and complexity of the machine tool is lower, compared to a parallel kinematic machine. Because of this, a serial setup was assumed to be mounted at the machine basis. Since the reused solution was created for a hexapod that has a parallel kinematic, the predicted losses would not be characteristic for an axis with a serial machine kinematic, not allowing a transfer of estimated losses. Therefore, the power loss prediction with the hexapod was performed without the hexapods kinematic transformation (on axis level). This forces

the VNC to ignore the axis setup of the hexapod and directly transfers positions to the physical axis, only considering the first 3 axes of the hexapod as it would be the X, Y and Z axis of a serial machine setup. With this adaption of the solution, the predictions become comparable to the assumed serial axis setup at the machine basis, which allows a transfer to the research object.

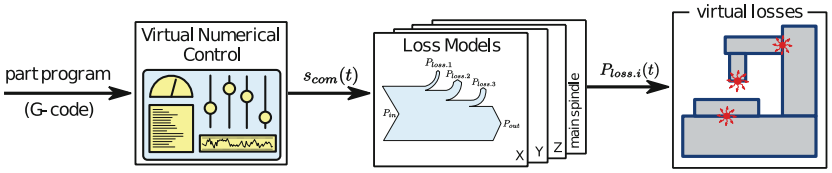

Fig. 9. Procedure for the prediction of task specific losses

4.3 Transformation of Thermal Loads

The machine basis has no lossy assemblies mounted that could introduce process dependent heat. Instead, 20 heating pads are mounted to mimic such losses (see Fig. 1 and 13). Therefore, an X-axis was assumed to be mounted in the centre of the machine basis, as illustrated at the bottom of Fig. 10. The loss prediction in the previews section was created for a hexapod without kinematic transformation (see top of Fig. 10 for axis setup). The predicted power losses for the hexapod are therefore comparable to a serial machine axis as assumed at the demonstrator. To transfer the losses from the hexapod axis to the demonstrator, the assembly characteristic losses are mirrored and scaled to the corresponding position of the assumed demonstrator axis (see Fig. 10). In the following is described how this transfer was achieved.

The loss simulation for the task of the previews section led to characteristic losses in the hexapods motor, bearing and ball screw drive (spindle nut contact). These losses will further be used for the assumed X-axis at the machine basis. The ball screw drive loss was not considered, since it leads to a heat introduction in the spindle and nut, which are not modelled and additional have no direct contact to the machine basis. Figure 11 shows the unmodified power loss predictions for the hexapod. Since the hexapod contains no profile rail guide power loss, this loss was separately modelled with the use of an empirical model [12]. Parameters are: power loss P, frictional force F, axis speed v, width of the rail guide b, preload force F_v and dynamic load rating C.

$$P(t) = F(t) \cdot v(t) = b \cdot 10^3 \cdot \left(0.46 + 66 \cdot \left(\frac{F_v}{C}\right)^{2.5} + \left(0.46 + 5.2 \cdot \left(\frac{F_v}{C}\right)\right) \cdot v(t)\right) \cdot v(t) \tag{2}$$

The axis speed $v(t)$ was obtained from the loss prediction and losses were computed for a rail guide with of $b = 40\,\text{mm}$ and a preload of $F_v/C = 0.075$. Figure 12 shows the resulting power loss for a single rail guide.

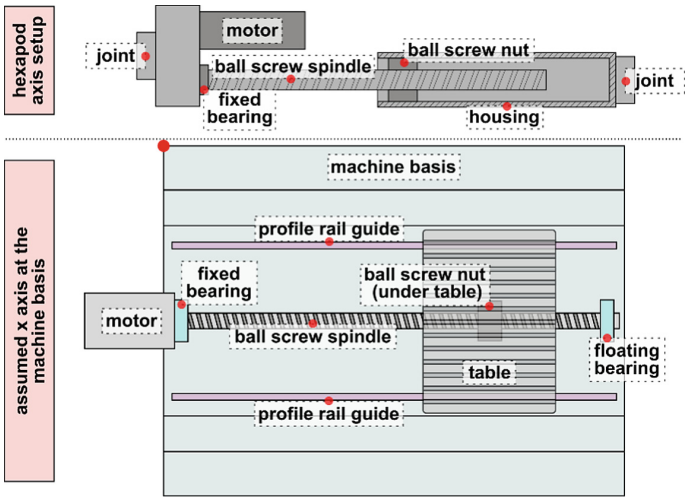

Fig. 10. Assumed constructive setup for thermal load transformation

A correlation between all curves can be seen, caused by the following general loss equation. Parameters are: power loss P, loss moment M, angular speed ω, loss force F, axis speed v and time t.

$$P(t) = M(t, \omega) \cdot \omega(t) = F(t, v) \cdot v(t) \tag{3}$$

Since $M \sim \omega$ and $F \sim v$, the power loss mainly depends on the activity (rotational speed ω or axis speed v) of the assembly, which can be expressed as $P \sim \omega^2 \sim v^2$ and reasons the obvious correlations of the curves.

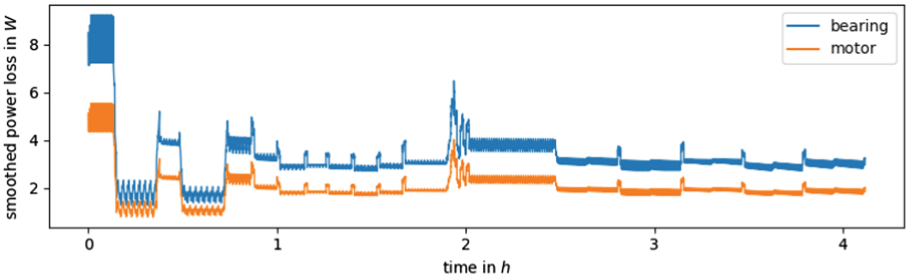

Fig. 11. Predicted power losses at the hexapod

At this point, all required characteristic power loss curves for lossy assemblies are defined. To mimic this relational behaviour with the heating pads, the curves need to be attached to the closest heating pads and a final normalisation over all curves is required, to obtain activity values within the range [0, 1] for direct application in the machine tool PLC (**P**rogrammable **L**ogical **C**ontroller) and the FEM. The attachment and resulting normalized curves are shown in Fig. 13b.

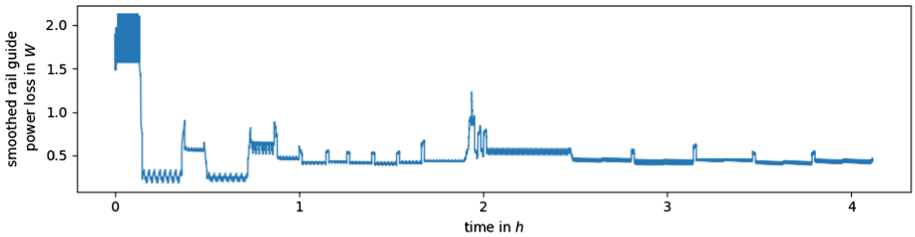

Fig. 12. Modelled power loss for a single profile rail guide

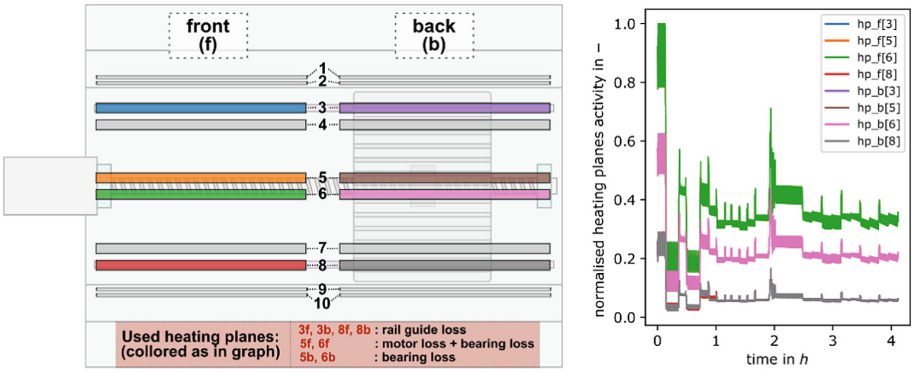

a) Heating pad positions with underplayed axis setup used for power loss assignment to specific pads

b) Derived heating pad activities

Fig. 13. Definition of realistic heating pad activities to mimic a real X-axis (Color figure online)

The attachment was performed manually by putting the assembly specific losses to the closest heating pad. Heating pad 5f and 6f are the closest to the fixed bearing and the motor. Therefore, both loss curves were added and equally divided to both heating pads. The floating bearing loss was attached to heating pads 5b and 6b. Profile rail guide losses were attached twice, once to heating pads 3f and 3b, and once to 8f and 8b. The position dependency was considered during loss assignment of the rail guide loss, by computing the absolute position of the front and back table edge, were a contact between table and rail guide was assumed. The loss got then attached to the closest heating pad, resulting in slight differences at the roughing operation, where it occurred that both contacts are closer to the front or back pad (see red curve under grey curve in Fig. 13).

5 Application and Evaluation of Dynamic Thermal Loads in FEM

The determined dynamic loads of the previous section are now applied to the machine basis and the FEM, to evaluate the forecast accuracy under dynamic thermal loads. First the application to the machine basis is described, followed by the application to the FEM. Finally, both results are compared and evaluated.

5.1 Dynamic Thermal Load Application to Machine Basis

Since Hydropol has a high heat capacity and a low conductivity, slow thermal changes arise as visible in Fig. 6 and 7, where even after 1 day no static temperature was reached. Therefore, the machine basis PLC was prepared to repetitively execute the thermal load scenario to get into the static state. This repetition mimics the conditions for manufacturing a batch of parts in a three-shift operation. Since a completion of one task requires a workpiece change and therefore a pause between two applications of the load scenario, a 10-min pause was added after each execution.

The measure was taken for one week, resulting in 40 measurements, one for each repetition. These measure represents the reference where the FEM will be compared to in Sect. 5.3. The measure includes the environmental temperature, which was measured by one sensor that was provided with fresh air by a fan. Inhomogeneity effects in environmental temperature could therefore not be detected, which for example could be caused by hall gates.

5.2 Dynamic Thermal Load Application in FEM

The load scenario was repetitively executed with a 10-min pause in between, for 40 times at the real machine basis. To simulate the same time with the FEM, a concatenation of the load scenario was performed, considering the 40 repetitions with 10-min pauses in between. The resulting CSV was passed to the FEM together with the optimized parameters and the simulation was started with a time step of 2 h. The simulation was completed after approximately half a day and will be compared with the measured behaviour in Sect. 5.3.

5.3 Comparison and Evaluation of Measured and Simulated Behaviour

The measured and simulated machine basis behaviour contains 30 temperature curves over one-week repetitive task application. Figure 14 shows an exemplary sensor and its measured and simulated temperature. Since a single discussion of all 30 temperature deviations would exceed the limits of this paper, some specific evaluations were performed to identify extremes and discuss them in detail. The equations are listed in the following. Parameters are: measured temperature series for a specific sensor T_{mea}, simulated temperature series for a specific sensor T_{sim}.

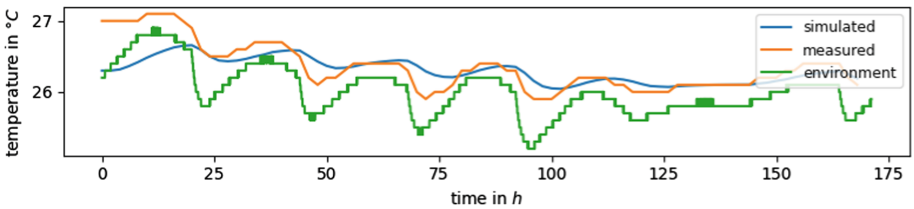

Fig. 14. Comparison of simulated and measured temperatures at sensor 3 (best correlation)

- Range of thermal change in measured behaviour ΔT_{mea}, which is further used as reference for relative error computation.

$$\Delta T_{mea} = \max(T_{mea}(t)) - \min(T_{mea}(t)) \tag{4}$$

- Mean error between measured and simulated sensor temperature E_m.

$$E_m = \overline{|\Delta T(t)|} = \overline{|T_{mea}(t) - T_{sim}(t)|} \tag{5}$$

- Relative error between measured and simulated behaviour E_r.

$$E_r = \frac{\overline{|\Delta T(t)|}}{\Delta T_{mea}} = \frac{\overline{|T_{mea}(t) - T_{sim}(t)|}}{\Delta T_{mea}} \tag{6}$$

Figure 15 shows these three quantities over the 30 sensors to give a general impression of the model accuracy (see Fig. 1b for sensor locations). Sensors 1 to 22 show a small relative error with about 20% deviation on average (see Fig. 14, which is representative for these sensors). Great relative errors with approximately 60% occurred at sensors 23 to 30. Globally this results in a mean relative error of 30% with a mean absolute error of 0.55 K. The biggest deviations occurred in the bottom of the basis, with a maximum relative error of 104% at sensor 26. Figure 16 shows the measurement and simulation for this sensor. A quite stable offset is visible, which may be caused by a thermal offset in the sensor. Additionally, the overall temperature change at this sensor is relatively small with 0.7 K, reasoning the great relative error at this sensor.

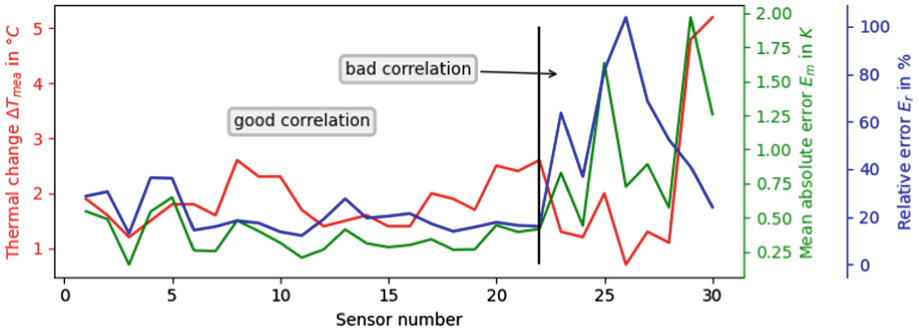

Fig. 15. Statistics of FEM

Overall can be said that the general accuracy of the model is quite accurate with a relative error of 30% and an absolute error of 0.55 K. The remaining error is assumed to be caused by the limited model capacity. A further error reduction should be possible by using a more detailed model. It is important to consider, that the model was only trained with one simple load scenario and can predict an untrained dynamic load scenario with no significant accuracy decrease. This shows that the consideration of task dependent loads, could improve thermal predictions in the field of machine tools.

The measures show one additional characteristic in the machine basis, that was already mentioned in Sect. 5.1: the slow thermal change. Figures 14 and 16 show the

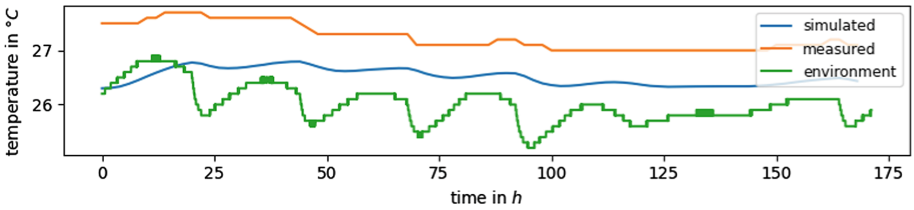

Fig. 16. Comparison of measured and simulated temperatures at sensor 26 (worst correlation)

thermal behaviour at specific positions in the machine basis, which is mainly dominated by the thermal change of the environment. The measures even show that the dynamics in environmental boundary conditions decrease at the weekend (hours 120 to 170 in Fig. 14 and 16), where no one is working.

The process itself is not directly visible, and mainly causing an offset between sensor temperature and environment. This makes short timed thermal simulations difficult, since past thermal loads influence the thermal starting condition. Such approaches are therefore difficult for small batch sizes, but can be valuable for large batch sizes, where quite static machine behaviour is achieved because of repetitive task execution.

6 Conclusion and Outlook

The paper issued the application of task dependent thermal loads in FEM simulations on the example of a machine basis. Section 3 showed the creation and parameter optimization for the FEM. With the use of APDL, the whole model could be runed and optimized by command line, which allows automation and could be valuable for the goals of digitalization, industry 4.0 or digital twins of machine tools [13]. Further the determination of task dependent thermal loads were presented in Sect. 4, which allows a more accurate consideration of thermal loads in FEM and with that increases the prediction accuracy. The whole procedure was applied and analysed in Sect. 5, were a good correlation between measure and simulation could be achieved.

It is important to consider that only one simple static load scenario was provided to optimize the FEM parameters. With this the model was capable to extrapolate from static loads to dynamic task dependent loads without an increase of the prediction error.

The overall model error is with 30% relatively high, but mainly caused by the simplified FEM, used in this research. Most limiting is the assumed homogeneous convection over all surfaces, not considered steel inlets and the rough model discretization. Further analyzations will therefore focus on the increase of model detail, to validate the expected increase in simulation accuracy.

Acknowledgements. The authors want to thank Framag Industrieanlagenbau GmbH [11] for providing the machine basis with integrated sensors and cooling circuits, the Hydac Cooling GmbH for providing the cooling aggregate as well as the German Research Foundation for funding the Project with Project-ID 174223256 – TRR 96.

References

1. Ramesh, R., Mannan, M.A., Poo, A.N.: Error compensation in machine tools – a review. Part I: geometric, cutting-force induced and fixture-dependent errors. Int. J. Mach. Tools Manuf. **40**(9), 1235–1256 (2000)
2. Möhring, H.C., Brecher, C., Abele, E., Fleischer, J.: Materials in machine tool structures. CIRP Ann. **64**(2), 725–748 (2015)
3. Voigt, I., Navarro de Sosa, I., Wermke, B., Bucht, A.: Increased thermal interia of ball screws by using phase change materials. Appl. Therm. Eng. **155**, 297–304 (2019)
4. Mori, K., Bergmann, B., Kono, D., Denkena, B., Matsubara, A.: Energy efficiency improvement of machine tool spindle cooling system with on-off control. CIRP J. Manuf. Sci. Technol. **25**, 14–21 (2019)
5. Shabi, L.: Thermo-Energetic Optimized Fluid Systems for Machine Tools. Dr.-Ing. Dissertation, Institute of Machatronic Engineering, TU Dresden (2019)
6. Weber, J., Steiert, C., Weber, J., Shabi, L.: Investigation of the thermal and energetic behavior and optimization towards smart fluid systems in machine tools. Procedia CIRP **99**, 80–85 (2021)
7. Schroeder, S., Kauschinger, B., Hellmich, A., Ihlenfeldt, S., Phetsinorath, D.: Identification of relevant parameters for the metrological adjustment of thermal machine models. Int. J. Interact. Des. Manuf. **13**(3), 873–883 (2019). https://doi.org/10.1007/s12008-019-00529-y
8. Naumann, C., et al.: Hybrid correction of thermal errors using temperature and deformation sensors. In: 1st Conference on Thermal Issues in Machine Tools, Dresden, Germany (2018)
9. Wenkler, E., Hellmich, A., Schröder, S., Ihlenfeldt, S.: Part program dependent loss forecast for estimating the thermal impact on machine tools. MM Sci. J. **3**, 4519–4525 (2021)
10. Wenkler, E., Selch, M., Hellmich, A., Ihlenfeldt, S.: Process concatenation to reduce thermal changes in machine tools. Int. J. Mechatron. Manuf. Syst. **15**(2–3), 167–184 (2022)
11. Hydropol® machine frames/machine beds. https://www.framag.com/en/products/hydropol-machine-frames-4621.html. Accessed 26 Sep 2022
12. Jungnickel, G.: Simulation des thermischen Verhaltens von Werkzeugmaschinen, Modellierung und Parametrierung, published by Großmann, K., TU Dresden, Dresden (2010)
13. Hänel, A., et al.: Digital twins for high-tech machining applications – a model-based analytics-ready approach. J. Manuf. Mater. Process. **5**(3), 80 (2021)